

Reduction of the return temperature in district heating systems with an ammonia-water absorption heat pump



N. Mirl*, F. Schmid, K. Spindler

Institute of Thermodynamics and Thermal Engineering (ITW), University of Stuttgart, Pfaffenwaldring 6, 70569 Stuttgart, Germany

ARTICLE INFO

Keywords:

Absorption heat pump
District heating system
Ammonia-water
Return temperature reduction
Exergetic efficiency

ABSTRACT

In this study, a new setup for the reduction of the return temperature in district heating systems will be presented. For this purpose, an ammonia-water absorption heat pump will be integrated within a district heating substation and theoretically investigated. The idea of this coupling is that the district heating flow is used to power the generator of the heat pump. The district heating return is cooled in the evaporator. In this way, the capacity of the district heating system can be increased or the mass flow rate can be reduced. Additionally, the lower return temperature leads to a higher efficiency of the whole system.

The field of possible operating points for such a system is also revealed and discussed.

1. Introduction

The temperature level of customer heating systems is subject to a constant change, e.g. due to decreasing heat consumption along with energy-efficiency retrofits or refurbishments of existing buildings. In district heating systems, however, higher operating temperatures and exergy levels are available. While, in customer heating systems, temperatures up to 70 °C are required for providing domestic hot water and room heating, temperatures range from 70 °C up to 140 °C in district heating systems in Germany [1]. An improved cooling of the district heating water leads to a reduction of the return temperature. Thus, heat distribution losses are reduced, the integration of low temperature (waste) heat sources are supported and the heat supply is increased [2,3]. It also allows to reduce the mass flow rate or increases the capacity of the district heating system significantly [4].

One opportunity to achieve these effects is to use the high temperature of the district heating flow to power an absorption heat pump with the working pair ammonia-water. After the cooling of the district heating water in a regular district heating substation, in the following referred as main heat exchanger, the return of the main heat exchanger can be used as heat source for the evaporator; leading to an improved cooling of the district heating water.

Due to the high corrosiveness of ammonia-water mixtures and the high system pressure, only stainless steel components with a pressure resistance of at least 30 bar at 150 °C should be used for the construction of an ammonia-water absorption heat pump. As long as the ammonia filling quantity is less than 10 kg, hardly any safety regulations for the place of installation of the heat pump have to be observed [5].

2. Process description and analysis

The schematic design of the district heating substation with an integrated absorption heat pump is shown in Fig. 1. The refrigerant

* Corresponding author.

E-mail address: nico.mirl@igte.uni-stuttgart.de (N. Mirl).

<https://doi.org/10.1016/j.csite.2018.10.010>

Received 14 May 2018; Received in revised form 27 September 2018; Accepted 27 October 2018

Available online 30 October 2018

2214-157X/ © 2018 The Authors. Published by Elsevier Ltd. This is an open access article under the CC BY-NC-ND license (<http://creativecommons.org/licenses/by-nc-nd/4.0/>).

Nomenclature		Subscripts	
c_p	specific heat capacity in $\text{kJ}\cdot(\text{kg}\cdot\text{K})^{-1}$	abs	absorber
\dot{E}	exergy change in kW	amb	ambient
h	specific enthalpy in $\text{kJ}\cdot\text{kg}^{-1}$	app	approach
\dot{M}	mass flow rate in $\text{kg}\cdot\text{s}^{-1}$	c	cooling
p	pressure in bar	CHS	customer heating system
P	electrical power in kW	cond	condenser
\dot{Q}	heat flow in kW	DHS	district heating system
s	specific entropy in $\text{kJ}\cdot(\text{kg}\cdot\text{K})^{-1}$	evap	evaporator
S	entropy in $\text{kJ}\cdot\text{K}^{-1}$	ex	exergetic
T	thermodynamic temperature in K	gen	generator
\dot{W}	heat capacity rate in $\text{kW}\cdot\text{K}^{-1}$	h	heating
$\Delta\theta$	temperature difference in K	high	high level
$\Delta\xi$	degassing range –	in	inlet
θ	temperature in $^\circ\text{C}$	low	low level
η	efficiency –	MHX	main heat exchanger
ζ	heat ratio –	out	outlet
ξ	mass fraction –	pump	circulating pump
Abbreviations		return	district heating return
RHX	refrigerant heat exchanger	SS	strong solution
SHX	solution heat exchanger	WS	weak solution

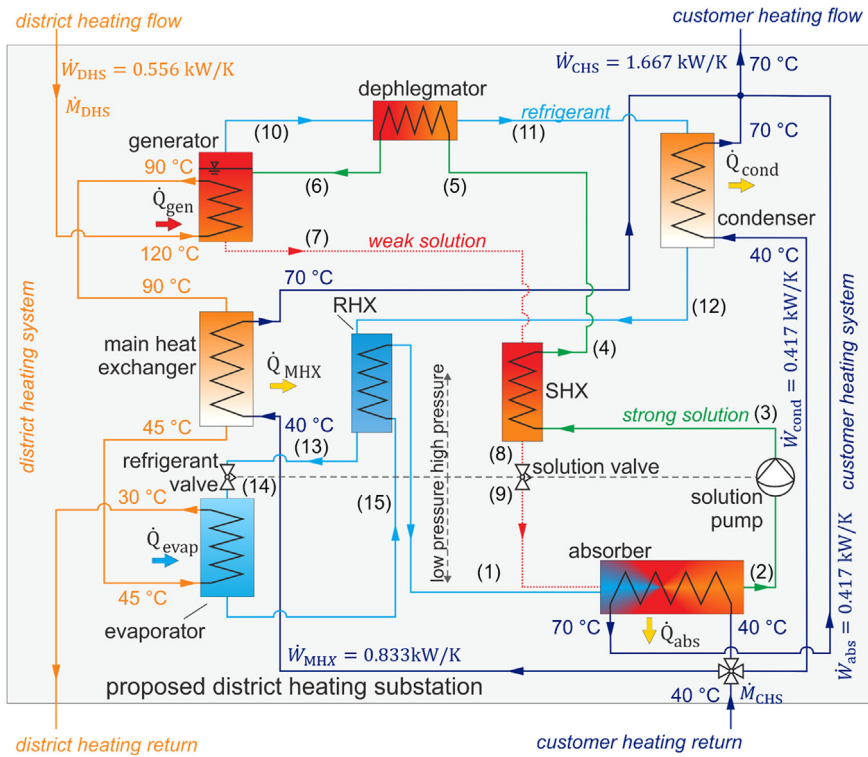


Fig. 1. Schematic design of the proposed district heating substation with integrated ammonia-water absorption heat pump with exemplary data.

ammonia is available in vapour phase (1). The refrigerant vapour is mixed with the weak solution (9) in the absorber, resulting in the refrigerant’s absorption. In this process, the heat of absorption Q_{abs} is released. Therefore, heat must be transferred to the customer heating system at a medium temperature level. At the end of the absorption process, the strong solution has an increased ammonia mass fraction ξ_{SS} and is in liquid state (2). Via a solution pump, the strong solution is adjusted to the high pressure (3).

The generator takes heat \dot{Q}_{gen} at a high temperature level from the district heating flow to separate the strong solution (6) into refrigerant vapour (10) and weak solution (7). The latter is fed back to the absorber and reused for the absorption process. In order to increase efficiency, a solution heat exchanger (SHX) is used for internal heat recovery between strong solution (3→4) and weak solution (7→8).

The refrigerant vapour extracted from the generator is no pure ammonia due to its thermodynamic equilibrium with the solvent water. In order to increase the refrigerant’s purity, the vapour is partially condensed in a dephlegmator. In this process, water is predominantly separated, accumulates in the liquid phase and is fed back to the generator. As heat sink for the dephlegmator, the strong solution at high temperature can be used for high exergetic efficiency (5→6) [6]. The refrigerant vapour (11) is liquefied in the condenser at the temperature level of the customer heating flow where another part of the useful heat is extracted from the process. Via an expansion valve, the liquid refrigerant’s pressure is reduced to the low pressure of the heat pump (13→14). At the low pressure, the refrigerant can be evaporated at a low temperature level (14→15). This effect is used to extract heat from the district heating return and thus to achieve the return temperature reduction. The refrigerant heat exchanger (RHX) is used to increase the efficiency in the process: the refrigerant vapour (15→1) is superheated and the liquid refrigerant is subcooled after the condenser (12→13).

As a result of the proposed coupling, the heat transferred to the evaporating refrigerant leads to the reduction of the district heating return temperature even below the customer heating return temperature. For illustration purpose, an example is discussed in the following sections.

2.1. Energy balance

The advantage of the given concept can be shown by the use of the exergetic efficiency as well as an energy balance for a heat loss free district heating substation. The heat input in the generator \dot{Q}_{gen} , in the evaporator \dot{Q}_{evap} , in the main heat exchanger \dot{Q}_{MHX} and the electrical power of the solution pump P_{pump} must be equal to the useful heat in the customer heating system. The latter is the sum of the transferred heat in the absorber \dot{Q}_{abs} , the condenser \dot{Q}_{cond} and the main heat exchanger \dot{Q}_{MHX} .

$$\dot{Q}_{MHX} + \dot{Q}_{gen} + \dot{Q}_{evap} + P_{pump} = \dot{Q}_{MHX} + \dot{Q}_{abs} + \dot{Q}_{cond} \tag{1}$$

To assess the efficiency of an absorption heat pump, the heat ratio ζ_h is defined as ratio of the useful heat of the heat pump to the heat needed at the generator. Neglecting the electrical power of the solution pump, the heat ratio can be rewritten as shown in Eq. (2).

$$\zeta_h = \frac{\dot{Q}_{abs} + \dot{Q}_{cond}}{\dot{Q}_{gen}} \approx 1 + \frac{\dot{Q}_{evap}}{\dot{Q}_{gen}} = 1 + \zeta_c \tag{2}$$

According to Eq. (2), the heat ratio of an absorption heat pump ζ_h is directly related to the heat ratio of an absorption chiller ζ_c . The latter results in the ratio of temperature differences in the district heating system by assuming a constant specific heat capacity c_p :

$$\zeta_c = \frac{\dot{Q}_{evap}}{\dot{Q}_{gen}} = \frac{\dot{M}_{DHS} \cdot c_p \cdot \Delta\vartheta_{DHS, evap}}{\dot{M}_{DHS} \cdot c_p \cdot \Delta\vartheta_{DHS, gen}} = \frac{\dot{W}_{DHS} \cdot \Delta\vartheta_{DHS, evap}}{\dot{W}_{DHS} \cdot \Delta\vartheta_{DHS, gen}} = \frac{\Delta\vartheta_{DHS, evap}}{\Delta\vartheta_{DHS, gen}} \tag{3}$$

In order to achieve a high reduction of the district heating return temperature, the temperature difference at the evaporator $\Delta\vartheta_{DHS, evap}$ has to be high. The heat ratio ζ_c depends on the specific operating point. According to Eq. (3), a high heat ratio ζ_c as well as

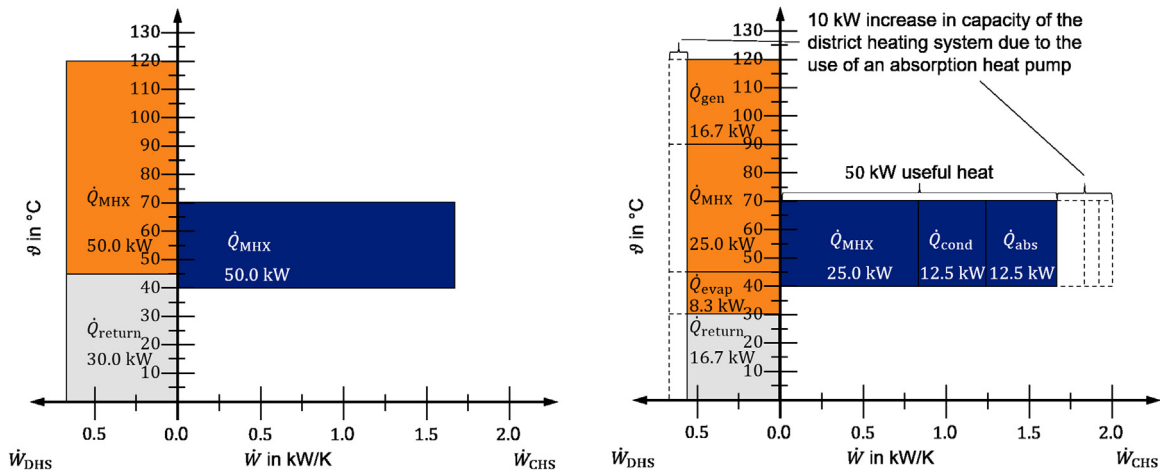


Fig. 2. Increase in capacity of the district heating substation due to the reduction of the district heating return temperature. The heat ratio of the absorption heat pump is assumed to be $\zeta_h = 1.5$.

a high temperature difference at the generator $\Delta\vartheta_{DHS,gen}$ are required for reaching a high temperature difference at the evaporator $\Delta\vartheta_{DHS,evap}$ and hence a high reduction of the district heating return temperature.

$$\dot{W} = \dot{M} \cdot c_p \tag{4}$$

A comparison of a generic operating point for a district heating substation, with and without absorption heat pump, is shown in Fig. 2. On the x-axis, the heat capacity rate \dot{W} as defined in Eq. (4) is shown. The fluid temperature ϑ is shown on the y-axis. The multiplication of the heat capacity rate \dot{W} with the temperature difference of the fluid $\Delta\vartheta$ results in the heat flow \dot{Q} transferred from or to the fluid. This correlation is used in Fig. 2 to illustrate the heat flows within the district heating substation. The useful heat of the district heating substation is set to be constant at 50 kW for both cases and corresponds to the heating capacity of the absorption system used in [6,7].

On the left of Fig. 2, the heat flow within a district heating substation without an absorption heat pump is illustrated. Due to the use of a non-ideal heat exchanger, the district heating return temperature $\vartheta_{DHS,MHX,out}$, e.g. 45 °C, is higher than the customer heating return $\vartheta_{CHS,in}$, e.g. 40 °C. Since there is no absorption heat pump integrated, the total heat flow \dot{Q}_{MHX} is transferred at the main heat exchanger.

On the right of Fig. 2, the combination with an absorption heat pump is illustrated. The heat ratio of the absorption heat pump is set to the value $\zeta_h=1.5$, which is less than the result of a first process simulation. The temperature of the district heating flow $\vartheta_{DHS,in} = \vartheta_{DHS,gen,in}$ is used to power the generator. The generator outlet temperature of the district heating system $\vartheta_{DHS,gen,out}$ is reduced to the temperature of the strong solution ϑ_s , e.g. 90 °C. Afterwards, the water of the district heating system is used to heat up the customer heating system direct within a main heat exchanger. At this point, the temperature in the district heating system $\vartheta_{DHS,MHX,out}$, e.g. 45 °C, is the same as in the left of Fig. 2. A further reduction of the return temperature takes place in the evaporator. As illustrated, the district heating return temperature $\vartheta_{DHS,evap,out}$, e.g. 30 °C, can be lower than the customer heating return temperature $\vartheta_{CHS,in}$, e.g. 40 °C. Since the additional heat transferred from the district heating system to the evaporator is also part of the useful heat, the mass flow and thus the heat capacity rate can be reduced by 20%. Otherwise, with the same mass flow rate of the district heating system, the capacity of the district heating system can be increased by 10 kW. As mentioned before, the lower district heating return temperature causes also lower distribution heat losses and a higher efficiency of the heat generation in a power plant.

2.2. Exergetic efficiency

The exergy change during a heat transfer process can be calculated by the use of Eq. (5).

$$\dot{E}_{12} = \dot{Q}_{12} - T_{amb} \cdot (S_2 - S_1) = \dot{M} \cdot [(h_2 - h_1) - T_{amb} \cdot (s_2 - s_1)] \tag{5}$$

For this analysis, the ambient temperature is set to 20 °C ($T_{amb} = 293.15$ K). The values for the enthalpy and entropy of water are calculated at a pressure of $p=5$ bar by the use of the Engineering Equation Solver (EES) [8,9]. The exergetic efficiency η_{ex} used in this work is defined as the exergy change of the customer heating system (CHS) divided by the exergy change of the district heating system (DHS):

$$\eta_{ex} = \frac{\dot{E}_{CHS}}{\dot{E}_{DHS}} \tag{6}$$

The results of these calculations are listed in Table 1 for the same operating point used in Fig. 2. Due to the use of an ammonia-water absorption heat pump with a heat ratio of $\zeta_h=1.5$, the exergetic efficiency increases by 12.7%. The required exergy for the heating of the building is still constant. The higher exergetic efficiency of the system is the result of the reduced district heating return temperature and thus a lower mass flow in order to keep the useful heat constant.

2.3. Operating points

An ammonia-water absorption heat pump can be used to reduce the return temperature of a district heating system $\vartheta_{DHS,out} = \vartheta_{DHS,evap,out}$. However, not every operating point is suitable for the use of an ammonia-water absorption heat pump. For this purpose, contour plots of possible operating points of the ammonia-water absorption heat pump and the theoretical achievable return

Table 1

Exergetic evaluation of the district heating substation with and without an absorption heat pump. The heat ratio of the absorption heat pump is assumed to be $\zeta_h=1.5$.

Without absorption heat pump		With absorption heat pump	
\dot{E}_{CHS}	5.302 kW	\dot{E}_{CHS}	5.302 kW
$\dot{E}_{DHS,gen}$	–	$\dot{E}_{DHS,gen}$	3.763 kW
$\dot{E}_{DHS,MHX}$	8.645 kW	$\dot{E}_{DHS,MHX}$	3.447 kW
$\dot{E}_{DHS,evap}$	–	$\dot{E}_{DHS,evap}$	0.466 kW
$\sum \dot{E}_{DHS}$	8.645 kW	$\sum \dot{E}_{DHS}$	7.676 kW
η_{ex}	0.613	η_{ex}	0.691

temperature reduction $\Delta\vartheta_{DHS, \text{evap}}$ are calculated and provided in Fig. 3. Each plot is valid for a specific inlet temperature at the generator. The generator inlet temperature $\vartheta_{DHS, \text{gen, in}}$ is varied between 80 °C and 120 °C. The combination of the inlet temperature at the absorber $\vartheta_{CHS, \text{abs, in}}$ and the outlet temperature at the condenser $\vartheta_{CHS, \text{cond, out}}$ are shown on the x-axis. On the y-axis, the inlet and outlet temperature at the evaporator $\vartheta_{DHS, \text{evap, in/out}}$ is shown.

This investigation is performed with the EES program. The properties of the ammonia-water mixture are calculated with the Helmholtz free energy equation of state by Tillner-Roth and Friend [10,11]. To create these plots, it is assumed that thermodynamic equilibrium is valid. The refrigerant is assumed to be pure ammonia. Therefore, the high pressure p_{high} of the heat pump can be calculated as the saturation pressure of the outlet temperature at the condenser. Furthermore, the low pressure p_{low} is calculated as the theoretical maximum pressure and thus the saturation pressure at the evaporator's outlet temperature $\vartheta_{DHS, \text{evap, out}}$. The ammonia mass fraction of the strong solution ξ_{SS} is calculated as saturated liquid with the use of the absorber's inlet temperature $\vartheta_{CHS, \text{abs, in}} = \vartheta_{CHS, \text{in}}$ and the low pressure p_{low} . The ammonia mass fraction of the weak solution ξ_{WS} is calculated as saturated liquid at high pressure p_{high} and the inlet temperature of the generator $\vartheta_{DHS, \text{gen, in}}$. If the resulting degassing range $\Delta\xi = \xi_{\text{SS}} - \xi_{\text{WS}}$ is negative, the operation of the ammonia-water heat pump will not be possible. To simplify handling, a resulting degassing range of $\Delta\xi=0$ is converted into a maximum possible temperature difference of the heat transfer. This temperature difference is referred in the following as approach temperature difference $\Delta\vartheta_{\text{app}}$ and is shown in Fig. 3 as colour gradient. It has been assumed, that the approach temperature difference $\Delta\vartheta_{\text{app}}$ is equal at the evaporator ($\vartheta_{DHS, \text{evap, out}} - \vartheta_{14}$), the absorber ($\vartheta_{CHS, \text{abs, in}} - \vartheta_2$) and the condenser ($\vartheta_{CHS, \text{cond, out}} - \vartheta_{11}$). However, the approach temperature difference at the generator $\Delta\vartheta_{\text{app, gen}} = \vartheta_{DHS, \text{gen, in}} - \vartheta_7$ is assumed to be $\Delta\vartheta_{\text{app, gen}} = 0\text{K}$.

Fig. 3 can be used to find the lowest possible evaporator outlet temperature $\vartheta_{DHS, \text{evap, out}}$ for a given generator inlet temperature $\vartheta_{DHS, \text{gen, in}}$, a given approach temperature difference $\Delta\vartheta_{\text{app}}$ and a given absorber inlet $\vartheta_{CHS, \text{abs, in}}$ and condenser outlet temperature $\vartheta_{CHS, \text{cond, out}}$. Case a) of Fig. 3 shows the operating point used before. The first point to be drawn into the diagram, results from the inlet temperature at the evaporator $\vartheta_{DHS, \text{evap, in}} = 45\text{ °C}$ and the flow and return temperatures of the customer heating system $\vartheta_{CHS, \text{abs, in}} = 40\text{ °C}$ and $\vartheta_{CHS, \text{cond, out}} = 70\text{ °C}$, respectively. For a known approach temperature difference $\Delta\vartheta_{\text{app}}$ between the heat exchanging fluids, the achievable outlet temperature at the evaporator $\vartheta_{DHS, \text{evap, out}}$ can be determined. Assuming idealized heat exchangers, the approach temperature difference is $\Delta\vartheta_{\text{app}} = 0\text{K}$. As a result, the minimum outlet temperature at the evaporator of the district heating circuit in case a) is $\vartheta_{DHS, \text{evap, out}} = 5\text{ °C}$, which is equal to the district heating return temperature $\vartheta_{DHS, \text{out}}$. Hence, the achievable district heating return temperature reduction is $\Delta\vartheta_{DHS, \text{evap}} = 40\text{ K}$. In case of an ammonia-water absorption heat pump with non-ideal heat exchangers, e.g. $\Delta\vartheta_{\text{app}} = 5\text{ K}$, the temperature reduction decreases to a remaining return temperature reduction of $\Delta\vartheta_{DHS, \text{evap}} = 27\text{ K}$.

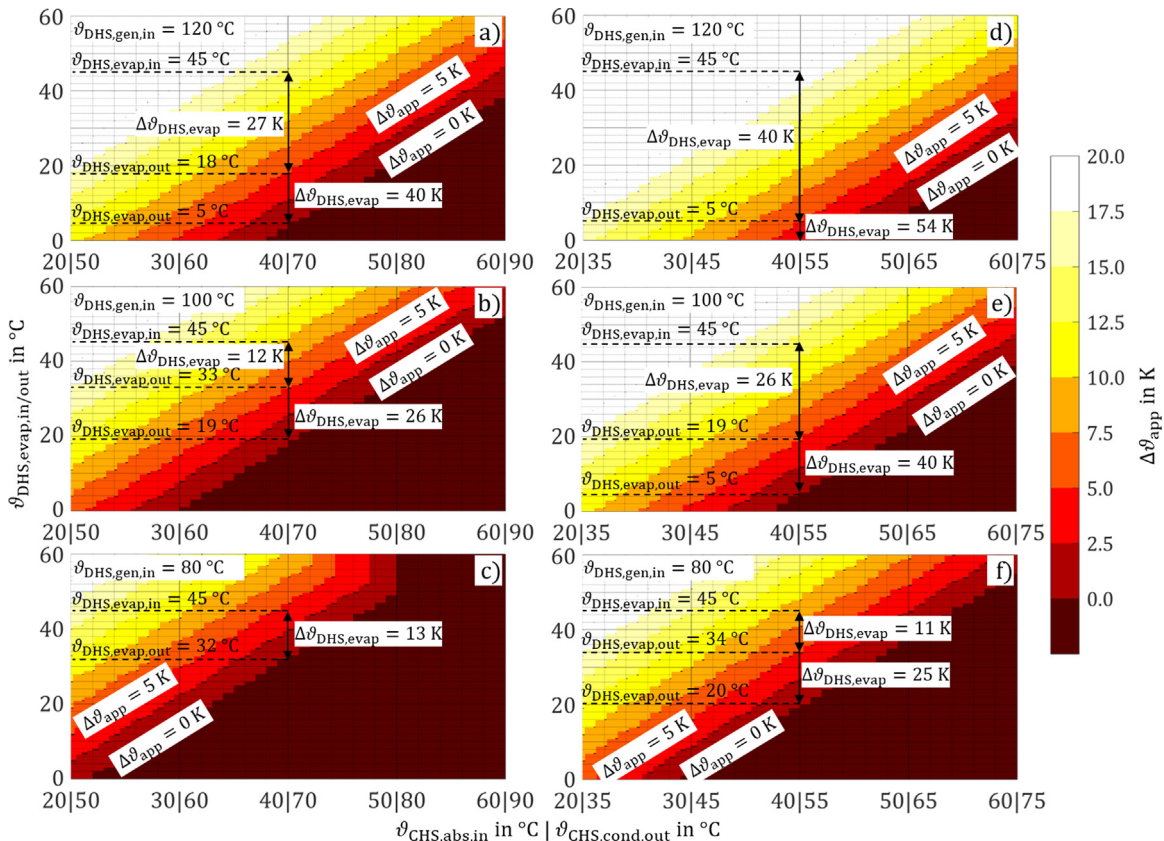


Fig. 3. Contour plots of possible operating points for an ammonia-water absorption heat pump and achievable district heating return temperature reduction.

This leads to an outlet temperature at the evaporator and thus to a district heating return temperature of $\vartheta_{\text{DHS,evap,out}} = 18^\circ\text{C}$.

In the cases b) and c) of Fig. 3, the district heating flow temperature $\vartheta_{\text{DHS,in}} = \vartheta_{\text{DHS,gen,in}}$ is decreased. This leads to an increase of the ammonia mass fraction of the weak solution ξ_{WS} and thus to a decrease in the degassing range $\Delta\xi$. Hence, the field of possible operating points as well as the achievable return temperature reduction $\Delta\vartheta_{\text{DHS,evap}}$ is decreased. As mentioned before, the approach temperature difference at the generator $\Delta\vartheta_{\text{app,gen}}$ is assumed to be zero and thus the temperature at the generator inlet $\vartheta_{\text{DHS,gen,in}}$ is used to calculate the ammonia mass fraction of the weak solution ξ_{WS} . Furthermore, cases b) and c) can also be used for the same operation point as case a) but with an approach temperature difference at the generator. Hence, Fig. 3b) is also valid for $\vartheta_{\text{DHS,gen,in}} = 120\text{ K}$ with an approach temperature difference at the generator $\Delta\vartheta_{\text{app,gen}} = 20\text{ K}$ and Fig. 3c) for $\Delta\vartheta_{\text{app,gen}} = 40\text{ K}$, respectively. The cases d) to f) of Fig. 3 are showing the operation within a customer heating system with a temperature difference between absorber inlet $\vartheta_{\text{CHS,abs,in}}$ and condenser outlet $\vartheta_{\text{CHS,cond,out}}$ of $\Delta\vartheta_{\text{CHS}} = 15\text{ K}$. The comparison of the cases a) and d), b) and e) as well as c) and f) show the effect of a decreased outlet temperature at the condenser $\vartheta_{\text{CHS,cond,out}}$, while the inlet temperature at the absorber $\vartheta_{\text{CHS,abs,in}}$ is constant. In case d), for instance, the achievable temperature reduction is $\Delta\vartheta_{\text{DHS,evap}} = 54\text{ K}$ for an approach temperature difference of $\Delta\vartheta_{\text{app}} = 0\text{ K}$ and thus the evaporator outlet temperature is $\vartheta_{\text{DHS,evap,out}} = -9^\circ\text{C}$. The decreased temperature at the outlet of the condenser decreases the systems high pressure p_{high} . This leads to a decrease of the ammonia mass fraction of the weak solution ξ_{WS} and thus to a higher degassing range $\Delta\xi$. Hence, the achievable return temperature reduction $\Delta\vartheta_{\text{DHS,evap}}$ increases with a decreasing customer heating flow temperature $\vartheta_{\text{CHS,out}} = \vartheta_{\text{CHS,cond,out}}$.

3. Conclusions

A new setup for the reduction of district heating return temperature is presented. The main advantage of such a system is that a district heating return temperature even below the customer heating return temperature can be achieved. In this way, the capacity of the district heating system can be increased or the mass flow rate and thereby the power consumption of the circulating pump can be reduced. It was also revealed that the coupling of an ammonia-water absorption heat pump with a district heating system can operate in a wide range of district and customer heating system conditions. However, the proposed district heating substation can achieve the highest return temperature reduction in cases where a high temperature of the district heating flow is used to power a low temperature customer heating system.

Acknowledgements

The work is based on a project (funding code “19696 N/2”), which is supported within the scope of the “program for promoting joint industrial research (IGF)” by the German Federal Ministry of Economic Affairs and Energy (Bundesministerium für Wirtschaft und Energie, BMWi) on the basis of a decision by the German Bundestag via the Federation of Industrial Research Associations (Arbeitsgemeinschaft industrieller Forschungsvereinigungen, AiF). In addition, the project is a cooperation with the district heating research institute (Fernwärme-Forschungsinstitut, FFI). The authors would like to sincerely thank for their support.

Conflict of interest

There is no conflict of interest.

References

- [1] A. Paar (Ed.), Transformationsstrategien von fossiler zentraler Fernwärmeversorgung zu Netzen mit höheren Anteilen erneuerbarer Energien: Endbericht, AGFW-Projektges, Frankfurt am Main, 2013.
- [2] D. Schmidt, A. Kallert, M. Blesl, S. Svendsen, H. Li, N. Nord, K. Sipilä, Low temperature district heating for future energy systems, *Energy Proced.* 116 (2017) 26–38.
- [3] G.K. Schuchardt, Energetische Analyse von Nahwärmenetzen unter Berücksichtigung des mikroskopischen thermohydraulischen Netzzustandes, Verlag Dr. Hut, München, 2017.
- [4] R. Knierim, Rücklauftemperatur: Ein ungehobener Schatz für Versorger und Kunden: Weitere Erlöse aus ungenutzter Wärmeenergie, *EuroHeat & Power* 36 (2007) 56–65.
- [5] Deutsches Institut für Normung (DIN), DIN EN 378-1, 2016th ed., Beuth Verlag, Berlin, 2017 (accessed 30 January 2018).
- [6] M. Zetzsche, Experimentelle Untersuchungen und regelungstechnische Optimierung einer Ammoniak/Wasser-Absorptionskältemaschine in Kombination mit einem solar angetriebenen Kühlsystem mit Eisspeicher. Dissertation, Stuttgart, 2012.
- [7] T. Koller, K. Spindler, H. Müller-Steinhagen, Experimental and theoretical investigations of solidification and melting of ice for the design and operation of an ice store, *Int. J. Refrig.* 35 (2012) 1253–1265.
- [8] S.A. Klein, EES manual, F-Chart Software (2017).
- [9] L. Haar, J.S. Gallagher, G.S. Kell, NBS/NRC steam tables, *Chem. Ing. Tech.* 57 (1984) 812.
- [10] R. Tillner-Roth, D.G. Friend, A helmholtz free energy formulation of the thermodynamic properties of the mixture {water + ammonia}, *J. Phys. Chem. Ref. Data* 27 (1998) 63–96.
- [11] H.-J. Kretzschmar, Property Library for Ammonia-Water Mixtures: LibAmWa, 2010.